Fabrication of Cu(II) based halobenzoate appended ladder polymers with efficient charge transport property

Sakhiul Islam,[a] Baishakhi Pal,[b] Samim Khan,[a] Suvendu Maity,[c] Sanobar Naaz, [a] Prasanta Ghosh,[d] Partha Pratim Ray,*[b] and Mohammad Hedayetullah Mir*[a]

[a]Department of Chemistry, Aliah University, New Town, Kolkata 700 156, India.

[b]Department of Physics, Jadavpur University, Jadavpur, Kolkata 700 032, India.

[c]Department of Chemistry, Jadavpur University, Jadavpur, Kolkata 700 032, India.

[d]Department of Chemistry, R. K. M. Residential College, Narendrapur, Kolkata 700 103, India.

To whom correspondence should be addressed. E-mails: partha@phys.jdvu.ac.inand chmmir@gmail.com

Supporting Information

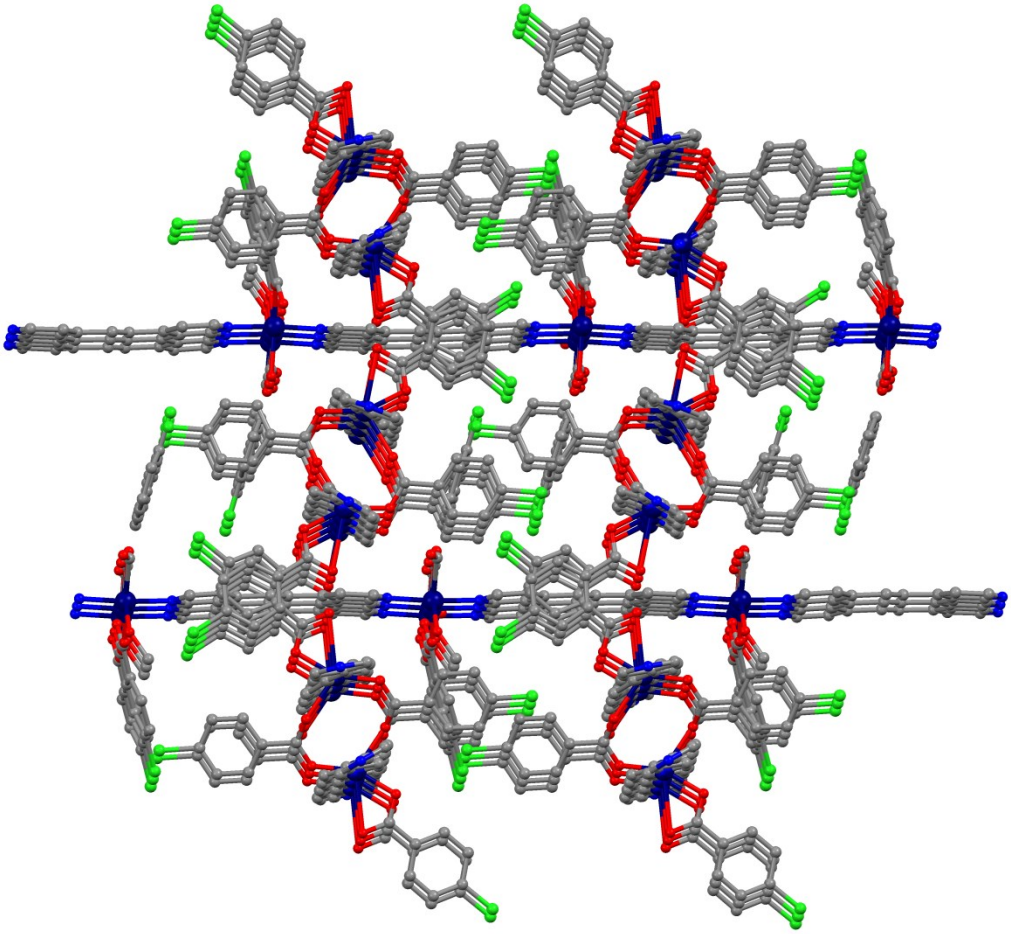

Fig. S1 3D supramolecular assembly formed via C-H···Cl, Cl···π and π···π stacking interactions in compound **1**.

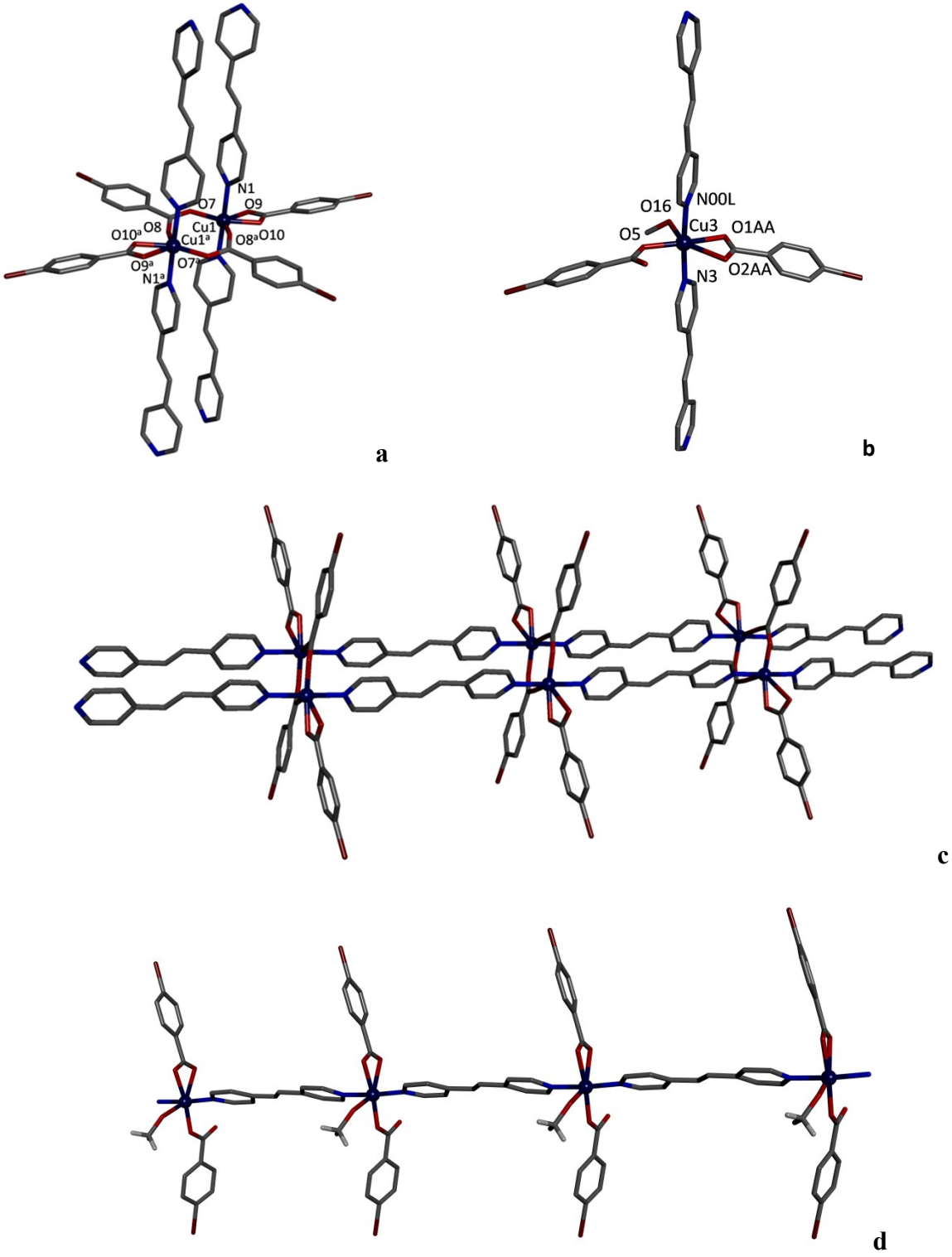

Fig. S2 Basic unit of (a) Cu(1) centre and (b) Cu(3) in compound **2**. Views of chain in Cu(1) (c) and Cu(3) (d) centres in **2**. Symmetry transformation a = 1-x, -y, 2-z.

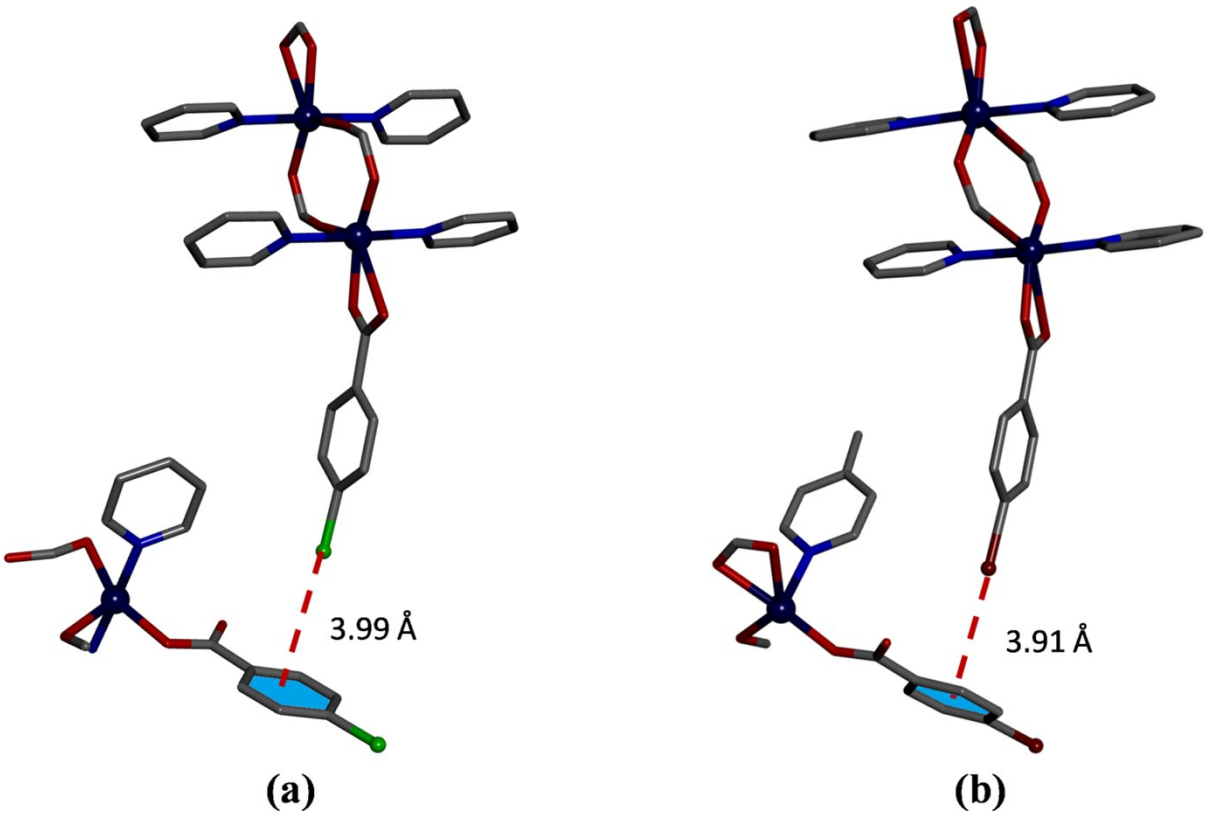

Fig. S3 Illustration of (a) Cl···π interaction in **1** and (b) Br···π interaction in **2**.

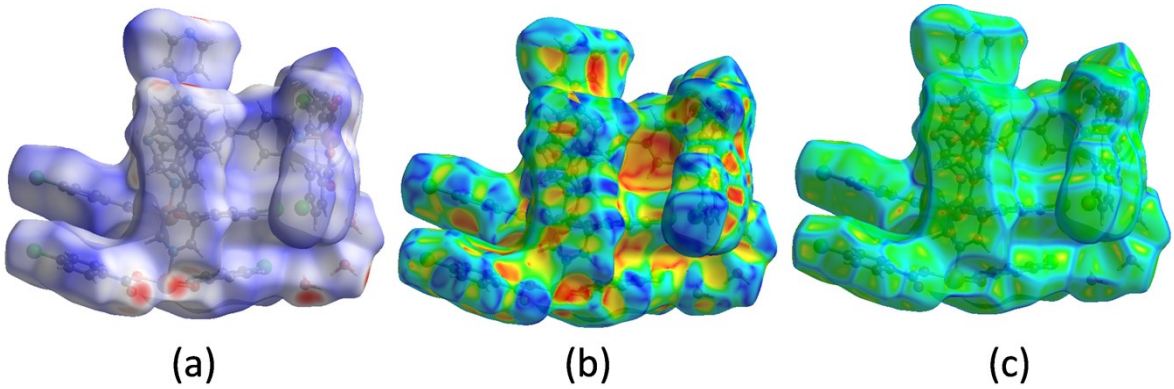

Fig S4. (a Hirshfeld surfaces mapped with dnorm (a), shape index (b) and curvedness (c) for compound **1**.

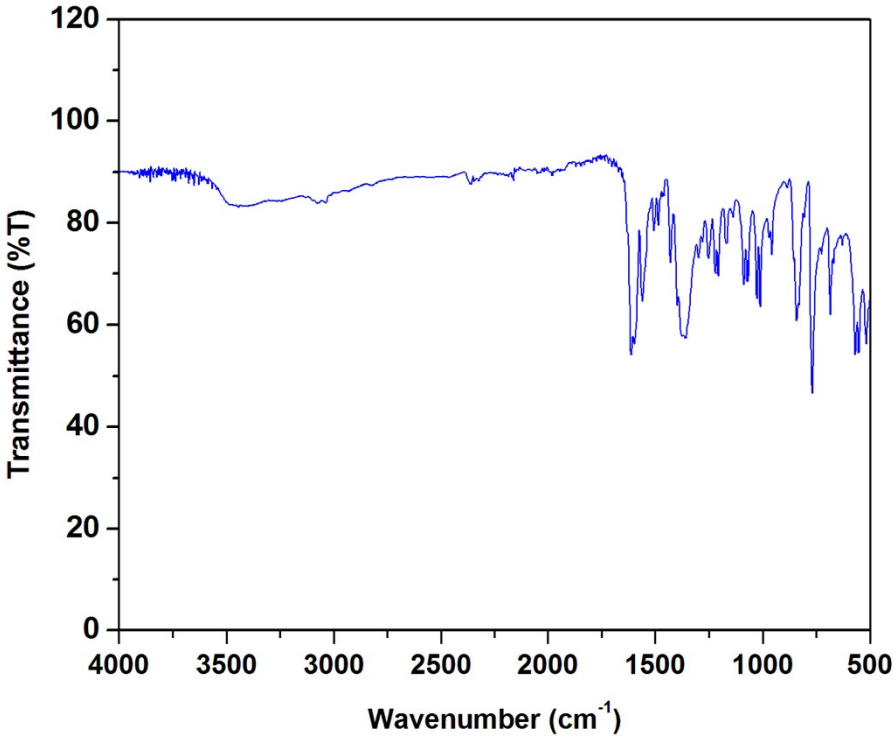

Fig. S5 IR spectrum of compound **1**.

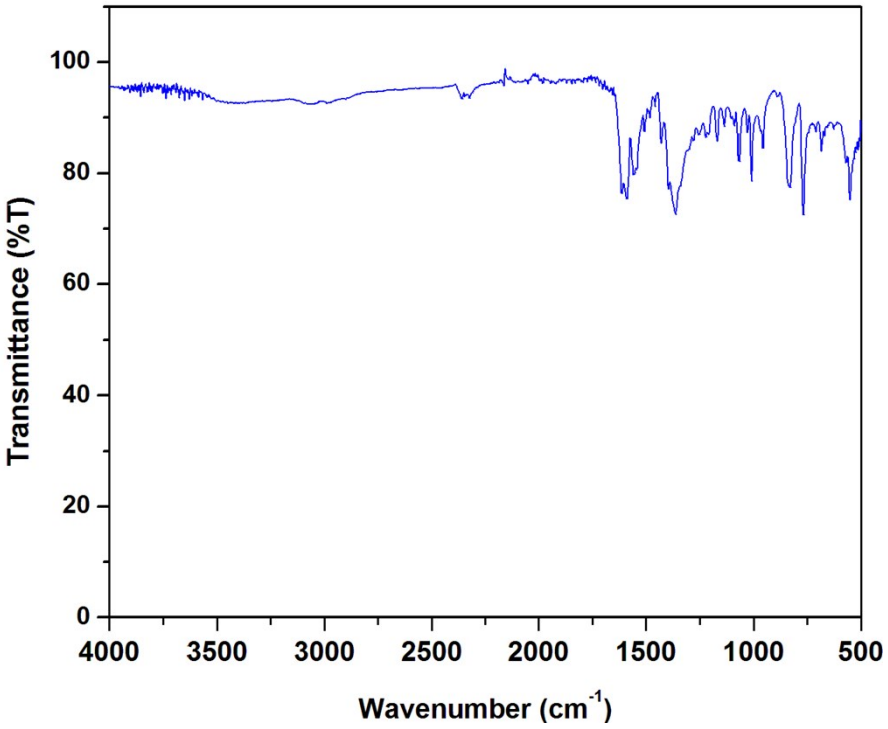

Fig. S6 IR spectrum of compound **2**.

Thermionic Emission theory:

According to Thermionic Emission theory, the forward bias current density can be expressed as

$$J = J_0\left[exp\left(\frac{q\,V}{\eta\,K\,T}\right) - 1\right] \quad (1)$$

When V=0, J=J_0=Saturation Current Density= $A^*T^2exp\left(-\frac{q\Phi_B}{KT}\right)$ (2)

Where, q=Electronic Charge, V=Applied Voltage, η= Ideality Factor, K=Boltzman's Constant, T=Temperature in Kelvin scale, Φ_B= Barrier potential Height, A^*= Rechardson's constant and was considered as 1.2×10^6 A m^{-2} K^{-2}.

Cheung's method:

According to Cheung's model, when a series resistance is designed as a series combination of resistor and diode, then the voltage across the diode can be substituted as the voltage drop across the series combination of diode and resistor. Then equation (1) can be drafted as,

$$J = J_0\left[exp\left(\frac{q\left(V - I\,R_S\right)}{\eta\,K\,T}\right)\right] \quad (3)$$

Where, IR_S term indicates the voltage drop across the series resistance of the semiconductor diode. Inserting the value of saturation current density into equation (3), and differentiate with respect to ln*J*, we get,

$$\frac{dV}{d\ln J} = A\,J\,R_S + \frac{\eta\,K\,T}{q} \quad (4)$$

Where, Rs=series resistance, q=Electronic Charge, η= Ideality Factor, K=Boltzman's Constant, T=Temperature in Kelvin scale

As stated in the Cheung model, the current density-reliant function H(J) can be written as,

$$H(J) = V - \frac{\eta K T}{q} \ln\left(\frac{J}{A^* T^2}\right) = A J R_S + \eta \Phi_B$$

(5)

Where, $\Phi_B =$ Barrier height, A*= Rechardson's constant and was considered as 1.2×10^6 A m^{-2} K^{-2}

Mott-Gurney equation:

Taking the slope of the *J* vs. V^2 graphs of region II, the effective interface mobility (μ_{eff}) of the charge carrier was estimated using Mott-Gurney space charge limited current density

$$J = \frac{9\ \mu_{eff}\ \varepsilon_0 \varepsilon_r}{8}\left(\frac{V^2}{d^3}\right) \quad (6)$$

ε_0 and ε_r is the dielectric permittivity of vacuum and dielectric constant of synthesized film respectively measured from capacitance (C)-frequency (f) curve shown in Fig. S6a and S6b. The relative dielectric constants of compound **1** and **2** were calculated to be 5.49 and 21.92, respectively.

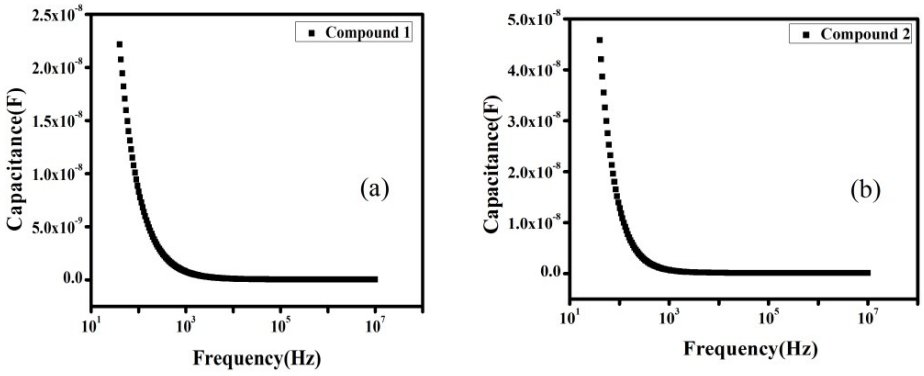

Fig. S7 Capacitance versus frequency plots for (a) compound **1** and (b) compound **2**.

From the saturation level of the curve of the Fig. S6a and S6b the dielectric permittivity of the semiconductor was evaluated by using eqn,

$$\varepsilon_r = \frac{1}{\varepsilon_0} \frac{C_{sat}\, d}{A} \tag{7}$$

Where d is the film thickness and A is the area of the diode.

$$\tau = \frac{9\, \varepsilon_0\, \varepsilon_r}{8\, d} \left(\frac{V}{J}\right) \tag{8}$$

The charge carrier concentration (N) was calculated using formula,

$$N = \frac{\sigma_{SCLC}}{q\, \mu_{eff}} \tag{9}$$

Where, σ_{SCLC} is the SCLC region conductivity.

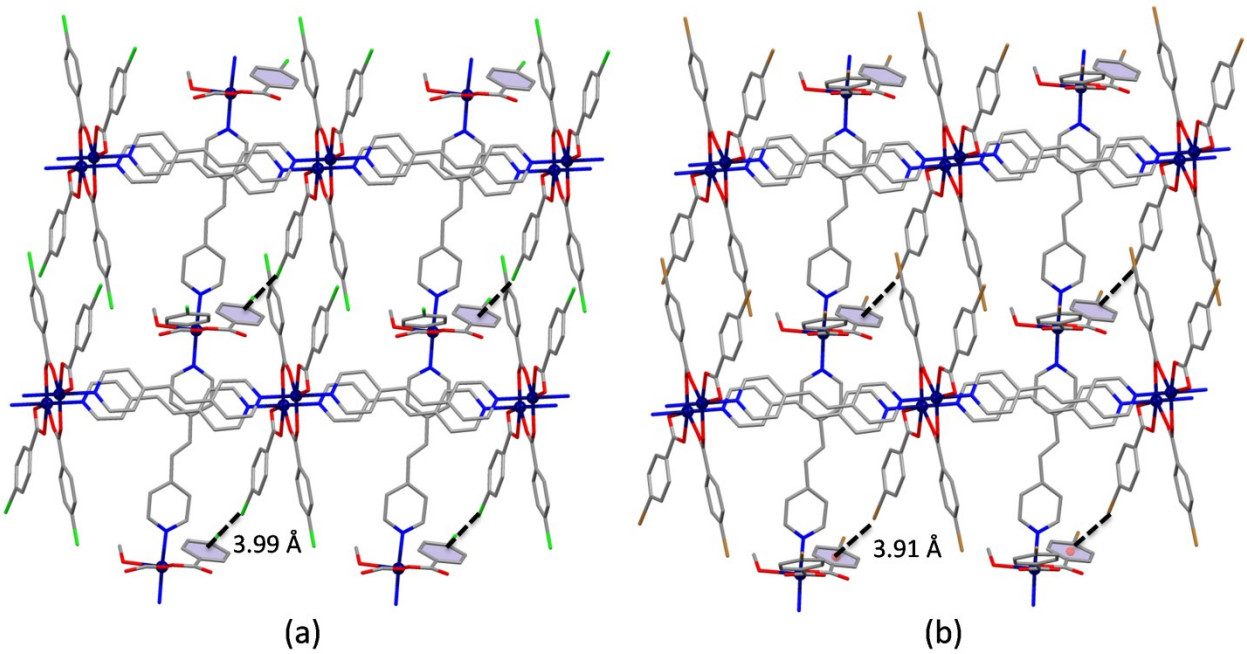

Fig. S8 Interlayer charge transport facilitated via halogen···π interactions in compound (a) **1** and (b) **2**.

Table S1: Crystal data and refinement parameters for compound **1** and **2**

Formula	$C_{79}H_{61}Cl_6Cu_3N_6O_{14}$ (**1**)	$C_{79}H_{60}Br_6Cu_3N_6O_{14}$ (**2**)
Fw	1721.69	1988.98
crystsyst	Triclinic	Triclinic
space group	*P*$\bar{1}$	*P*$\bar{1}$
a (Å)	13.3784(10)	13.3854(7)
b (Å)	13.4372(10)	13.4317(7)

c (Å)	22.8411(17)	23.0860(12)
α(deg)	79.854(4)	79.506(3)
β(deg)	86.664(4)	86.899(3)
γ (deg)	82.954(3)	84.385(2)
V (Å^3)	4008.6(5)	4058.8(4)
Z	2	2
D_{calcd}(g/cm^3)	1.426	1.628
μ(mm^{-1})	1.054	3.797
λ(Å)	0.71073	0.71073
GOF on F^2	1.041	1.058
final R indices[$I > 2\sigma(I)$][a,b]	$R1$ = 0.1113	$R1$ = 0.0734
	$wR2$ = 0.2673	$wR2$ = 0.2426

[a]$R1 = \Sigma||F_o| - |F_c||/ \Sigma|F_o|$, [b]$wR2 = [\Sigma w(F_o^2 - F_c^2)^2/\Sigma w(F_o^2)^2]^{1/2}$

Table S2: Selected bond lengths and bond angles in **1**

Cu(2)-O(2)	1.944(6)	Cu(2) -O(3)	1.987(7)
Cu(2) –O(4)	2.708(9)	Cu(2) -N(3)	2.032(7)
Cu(2)-N(4)[a]	2.038(7)	Cu(2)-O(1)_c	2.263(7)
Cu(1)-O(5)	1.985(7)	Cu(1)-O(6)	2.756(9)
Cu(1) -O(7)	1.944(7)	Cu(1)-N(1)	2.031(8)

Cu(1)-N(2)[d]	2.024(8)	Cu(1)-O(8)_f	2.310(9)
Cu(3)-N(5)	2.021(7)	Cu(3) -O0AA	2.129(14)
Cu(3) –O(10)	1.975(7)	Cu(3)-O(18)	2.394(9)
Cu(3)-N(6)[h]	1.996(7)	Cu(3)-C0AA	1.96(2)
Cu(3) –C(1)AA	2.56(2)	O(2)-Cu(2)-O(3)	154.8(3)
O(2)-Cu(2)-O(4)	101.8(3)	O(2) -Cu(2)-N(3)	86.9(3)
O(2)-Cu(2)-N(4)[a]	92.6(3)	O(1)c-Cu(2)-O(2)	117.9(3)
O(3) -Cu(2)-O(4)	53.6(3)	O(3) -Cu(2)-N(3)	88.4(3)
O(3) –Cu(2)-N(4)_a	92.5(3)	O(1)-Cu(2)-O(3)	86.7(3)
O(4)-Cu(2)-N(3)	91.1(3)	O(4) -Cu(2) -N(4)_a	90.0(3)
O(1)c-Cu(2)-O4	140.3(2)	O(4)-Cu(2)-N(3)	91.1(3)
N(3) -Cu(2)-N(4)_a	178.9(3)	O(1)_c-Cu(2)-N(3)	89.1(3)
O(1)_c-Cu(2)-N(4)_a	90.4(3)	O(6)-Cu(1)-N(1)	88.2(3)
O(6 -Cu(1)-N(2)_d	94.6(3)	O(6)-Cu(1) -O(8)_f	137.5(3)
O(7) -Cu(1)-N(1)	89.7(3)	O(7) –Cu(1)-N(2)_d	90.6(3)
O(7) -Cu(1)-O(8)_f	120.9(3)	N(1)-Cu(1)-N(2)_d	177.1(4)
O(8)_f -Cu(1)-N(1)	87.6(3)	O(8)_f-Cu(1)-N(2)_d	89.8(3)
O(5)-Cu(1)-N(1)	89.8(3)	O(5)-Cu(1)-O(6)	52.4(3)
O(5)-Cu(1)-O(7)	153.8(3)	O(6) -Cu(1)-O(7)	101.4(3)

Symmetry Code: [a] = x,-1+y,z;b= x,1+y,z;c= -x,-y,2-z;d= x,-1+y,z;f= -x,1-y,1-z

Table S3: Selected bond lengths and bond angles in **2**

Cu(1)-N(1)	2.029(5)	Cu(1)-O(9)	2.679(7)
Cu(1)-O(10)	1.976(4)	Cu(1)-O(7)	1.943(4)
Cu(1)-N(2)_a	2.016(5)	Cu(1)-O(8)_c	2.267(4)
Cu(2)-N(5)_d	2.036(6)	Cu(2)-O(3)	1.942(5)
Cu(2)-O(1)	1.973(5)	Cu(2)-N(4)	2.028(6)

Cu(2)-O(2)	2.744(7)	Cu(2)-O(4)_f	2.318(7)
Cu(3)-N00L	2.009(5)	Cu(3)-O(5)	1.966(4)
Cu(3)-N(3)_g	2.013(5)	Cu(3)-O(16)	2.408(6)
Cu(3) -O(11)	2.460(9)	O(7)-Cu(1)-O(9)	101.65(18)
O(7) -Cu(1) -O(10)	154.66(19)	O(7)-Cu(1)-N(1)	86.8(2)
O(7)-Cu(1)-N(2)_a	92.4(2)	O(7)-Cu(1)-O(8)_c	118.12(17)
O(9) -Cu(1)-O(10)	53.59(17)	O(9) –Cu(1)-N(1)	91.2(2)
O(9 -Cu(1)-N(2)_a	90.2(2)	O(8)_c -Cu(1)-O(9)	140.19(16)
O(10) -Cu(1)-N(1)	88.31(19)	O(10 -Cu(1) -N(2)_a	92.94(19)
O(8)_c -Cu(1)-O(10)	86.64(17)	N(1) –Cu(1)-N(2)a	178.54(19)
O(8)_c-Cu(1) -N(1)	89.23(19)	O(8)-Cu(1) –N(2)_a	90.11(19)
O(2) -Cu(2)-N(4)	85.6(2)	O(2) –Cu(2) -N(5)_d	97.6(2)
O(2)-Cu(2)-O(4)_f	138.47(19)	O(3) -Cu(2)-N(4)	90.4(2)
O(3) -Cu(2)-N(5)d	89.3(2)	O(3)-Cu(2)-O(4)f	119.5(2)
N(4) -Cu(2) -N(5)_d	176.9(3)	O(4)f-Cu(2)-N(4)	89.1(2)
O(4_)f-Cu(2)-N(5)_d	88.3(2)	O(1)-Cu(2)-N(4)	90.0(2)
O(1) -Cu(2)-O(2)	52.45(18)	O(1) –Cu(2)-O(3)	154.0(2)
O(2) -Cu(2)-O(3)	101.72(18)	O(1) -Cu(2)-N(5)d	91.7(2)
O(1)-Cu(2)-O(4)_f	86.5(2)	O(11) –Cu(3)-N00L	90.7(3)
O(16) -Cu(3)-N00L	92.7(2)	O(16) -Cu3 -N(3)_g	91.5(2)
N00L-Cu(3)-C02I	91.2(2)	N00L -Cu(3) –N(3)g	174.8(2)
O(11)-Cu(3)-N3_g	84.0(3)	O(12)-Cu(3)-N00L	89.4(3)
O(5)-Cu(3)-O(11)	132.1(3)	O(5) -Cu(3) -C02I	158.8(3)

Symmetry Code: a = x,-1+y,z; b = x,1+y,z;c=1-x,-y,2-z;d=x,-1+y,z;f=1-x,1-y,1-z;g=-1+x,y,z;i=-1+x,y,z;l=x,-1+y,z.

Table S4. Comparison of electrical conductivity data of some related CPs.

Compound	**Electrical Conductivity (S m^{-1})**	**References**
$[Cd(adc)(4\text{-phpy})_2(H_2O)_2]$, (1)	3.88×10^{-10}	1
$[Zn(adc)(4\text{-phpy})_2(H_2O)_2]$	1.52×10^{-10}	1
$[Cd\text{-}(quin)_2(4\text{-nvp})_2]$	7.36×10^{-5}	2
$[Zn(adc)(4\text{-spy})_2(H_2O)_2]_n$	16.48×10^{-4}	3
$[Zn_6(bpd)_3(p\text{-clba})_6(\mu_3\text{-}OH)_4].(p\text{-clba})_2.(CH_3OH)$	3.29×10^{-4}	4
$[Zn_6(bpd)_3(p\text{-brba})_6(\mu_3\text{-}OH)_4].(p\text{-brba})_2.(CH_3OH)$	2.22×10^{-4}	4
$[Zn(INH)(succ)]_n$	2.26×10^{-4}	5
$[Zn(INH)(fum)]_n$	1.12×10^{-4}	5
$[Zn(INH)(bdc)]_n$	1.25×10^{-4}	5
$\{[Cd_2(adc)_2(4\text{-nvp})_6]\cdot(MeOH)\cdot(H_2O)\}_n$	6.91×10^{-4}	6
$[\{Cu_2(p\text{-clba})_4(bpe)_2\}\{Cu(p\text{-clba})_2(bpe)(CH_3OH)\}]_n\cdot 1.25H_2O$	1.16×10^{-5}	**Compound 1**
$[\{Cu_2(p\text{-brba})_4(bpe)_2\}\{Cu(p\text{-brba})_2(bpe)(CH_3OH)\}]_n\cdot 1.25H_2O$	8.85×10^{-4}	**Compound 2**

References

1. F. Ahmed, J. Datta, B. Dutta, K. Naskar, C. Sinha, S. M. Alam, S. Kundu, P. P. Ray and M. H. Mir, *RSC Adv.*, 2017, **7**, 10369.
2. B. Dutta, A. Dey, C. Sinha, P. P. Ray and M. H. Mir, *Inorg. Chem.*, 2019, **58**, 5419−5422.

3. B. Dutta, A. Dey, K. Naskar, S. Maity, F. Ahmed, S. Islam, C. Sinha, P. Ghosh, P. P. Ray and M. H. Mir, *New J.Chem.,* 2018, **42**, 10309.

4. S. Islam, J. Datta, F. Ahmed, B. Dutta, S. Naaz, P. P. Ray and M. H. Mir, *New J. Chem.,* 2018, **42**, 13971.

5. K. Naskar, A. Dey, B. Dutta, F. Ahmed, C. Sen, M. H. Mir, P. P. Roy and C. Sinha, *Cryst. Growth Des.,* 2017, **17**, 3267.

6. B. Dutta, R. Jana, A. K. Bhanja, P. P. Ray, C. Sinha and M. H. Mir, *Inorg. Chem.*, 2019, **58**, 2686-2694.